Optimal Heading Change with Minimum Energy Loss for a Hypersonic Gliding Vehicle

Anthony J. Calise* and Gyoung H. Bae†
Georgia Institute of Technology, Atlanta, Georgia 30332

A three-state model is presented for analyzing the problem of optimal changes in heading with minimum energy loss for a hypersonic gliding vehicle. A further model order reduction to a single-state model is examined using singular-perturbation theory. The optimal solution for the reduced problem defines an optimal altitude profile dependent on the current energy of the vehicle. A separate boundary-layer analysis is used to account for altitude and flight-path angle dynamics and to obtain lift and bank-angle control solutions. By considering alternative approximations to solve the boundary-layer problem, three guidance laws are obtained, each having a feedback form. The guidance laws are evaluated for a hypothetical vehicle and are compared to an optimal solution obtained using a multiple shooting algorithm.

Nomenclature

C = characteristics velocity
C_L = lift coefficient
C_D = drag coefficient
C_{D0} = zero-lift drag coefficient
E = mass specific energy
h = altitude
H = Hamiltonian
K = induced drag coefficient
m = mass
r = radius from Earth center
S = reference area
t = time
V = velocity
β = scale height
γ = flight-path angle
$\delta( )$ = perturbation in ( )
ϵ = perturbation parameter
λ = normalized lift coefficient (C_L/C_L^*)
$\lambda_{( )}$ = costate variable associated with ( )
μ = bank angle
ν = gravitational constant
ρ = air density
τ = stretched time scale $(\tau = t/\epsilon)$
ψ = heading

Superscripts

$*$ = value at maximum lift/drag
o = reduced solution
$\bar{}$ = equilibrium value
$'$ = $d/d\tau$

Subscripts

c = value at initial circular orbit
BL = boundary layer
o = reduced solution
s = value at mean sea level

Received March 11, 1988; revision received March 27, 1989.

*Professor, Aerospace Engineering. Associate Fellow AIAA.
†Graduate Research Assistant, Aerospace Engineering.

Introduction

THIS paper addresses the problem of developing analytical methods for optimal guidance of hypersonic vehicles. Energy state approximations combined with singular-perturbation theory (SPT) have proved useful in aircraft trajectory optimization, both in obtaining algebraic control solutions and in satisfying trajectory and control constraints.[1-4] However, the underlying flat Earth and constant gravitational field assumptions in aircraft modeling do not apply to hypersonic vehicles. Moreover, the use of SPT requires an inherent time-scale separation in the problem formulation for successful application. It is not known at this time if SPT can be applied to hypersonic vehicle control optimization. The intent of this paper is to explore this possibility for a simple problem formulation.

The problem of optimal atmospheric heading change with minimum energy loss has application to maneuvering re-entry vehicle guidance and to aeroassisted orbit transfer vehicles (AOTV's). In this simple problem formulation, we ignore terminal constraints on both altitude and flight-path angle and thus avoid the issue of a terminal boundary-layer correction in these state variables. There is still a terminal boundary layer associated with their respective costate variables. However, the numerical results shown here indicate that these are of minor importance in an optimal re-entry problem. Comparisons can be made to the initial portion of an AOTV optimal maneuver and to the general characteristics of these optimal profiles.[5] References 6-8 typify the studies that have been performed on the problem of optimal aero-assisted orbital plane change. For circular orbits of nearly equal radii, it can be shown that fuel consumption is minimized by minimizing the energy loss in the atmospheric portion of the trajectory.

This paper presents a problem formulation suitable for singular-perturbation (SP) analysis. The reduced and boundary-layer solutions are examined and compared to numerical optimal solutions obtained using a multiple shooting algorithm,[9] and to the general characteristics of the numerical solutions given in Ref. 8 for the AOTV problem. By considering alternative approximations to solve the boundary-layer problem, three guidance laws are obtained, each having a feedback form. An evaluation of the first guidance law for use in an AOTV maneuver can be found in Ref. 10.

Problem Formulation

In Ref. 8, it has been shown that the cross-range angle for the orbital plane change trajectory that minimizes energy loss is negligibly small. With this approximation, the equations of

motion for flight over a nonrotating spherical Earth reduce to the following four-state model:

$$\dot{h} = V \sin\gamma \tag{1}$$

$$\dot{E} = -C_D^* S(1+\lambda^2)\rho V^3/4m \tag{2}$$

$$\dot{\gamma} = (C_L^* \rho SV/2m)(\lambda \cos\mu + M \cos\gamma) \tag{3}$$

$$\dot{\psi} = C_L^* \lambda \rho SV \sin\mu/2m \cos\gamma \tag{4}$$

where

$$C_D = C_{D0} + KC_L^2 \tag{5}$$

$$M(h,V) = (2m/C_L^* S)[1 - \nu/V^2 r]/\rho r, \qquad r = r_s + h \tag{6}$$

In these equations, the superscript asterisk denotes the maximum lift-to-drag values:

$$C_L^* = (C_{D0}/K)^{1/2}, \qquad C_D^* = 2C_{D0} \tag{7}$$

and λ is the normalized lift coefficient

$$\lambda = C_L/C_L^* \tag{8}$$

Here we have employed E as a state variable in place of velocity V, where

$$E = V^2/2 - \nu/r \tag{9}$$

In Ref. 8, velocity V is used as a state variable, and the gravity component was ignored in the velocity rate equation. One advantage to using E as a state variable is that Eq. (2) is independent of γ. In Eq. (9), the reference point for zero potential energy is taken at $r = \infty$. This transformation implies that wherever V appears in the equations, it is replaced by $[2(E + \nu/r)]^{1/2}$. The control variables are λ and the bank angle μ. Under the hypothesis that the cross-range angle is small, ψ closely approximates the change in orbit inclination.

Boundary Conditions

In Ref. 8, the sensible atmosphere is assumed to occur at $h(0) = 200{,}000$ ft. The starting velocity and flight-path angle are derived using a deorbit impulse ΔV_1 from circular orbit at $h_c = 100$ n.mi., which is optimized for the atmospheric maneuver of interest. The initial heading angle is taken as zero. In the SPT formulation, altitude appears as a control variable in the reduced problem. The optimal solution appears in the form

$$h^* = h_o(E) \tag{10}$$

For comparison purposes, in this paper, the starting energy is chosen to match that of Ref. 8 for the case of a 40-deg heading change. From conservation of energy, this results in the same deorbit impulse. The initial flight-path angle is derived from conservation of angular momentum.

$$\gamma(0) = -\cos^{-1}\left\{(r_c)(V_c - \Delta V_1)/[r_s + h(0)V(0)]\right\} \tag{11}$$

where r_c is the circular orbit radius and $V_c = (\nu/r_c)^{1/2}$ is the circular velocity. The vehicle begins the maneuver with a mass m_c and, as a result of the deorbit impulse, the mass for the atmospheric portion is given by

$$m = m_c \exp(-\Delta V_1/C) \tag{12}$$

The terminal condition is taken as

$$\psi(t_f) = \psi_f > 0 \tag{13}$$

There are no terminal constraints on altitude and flight-path angle; thus, their corresponding costate values are zero at the final time.

Optimal Control Problem

The objective is to minimize the energy lost in maneuvering to a specified heading. Regarding energy as a slow variable, and altitude and flight-path angle as fast variables, the following three state model was adopted for singular-perturbation analysis:

$$\dot{\psi} = C_L^* \rho SV\lambda \sin\mu/2m \cos\gamma \tag{14}$$

$$\epsilon\dot{h} = V \sin\gamma \tag{15}$$

$$\epsilon\dot{\gamma} = C_L^* \rho SV(\lambda \cos\mu + M \cos\gamma)/2m \tag{16}$$

The objective is to minimize

$$J = -\int_0^{t_f} \dot{E}\, dt \tag{17}$$

where

$$\dot{E} = -C_D^*(1+\lambda^2)\rho SV^3/4m \tag{18}$$

Note that in the preceding formulation, E is approximated as constant in the dynamics but that changes in energy are accounted for in the performance index. This approximation will later be relaxed in the subsequent analysis. The perturbation parameter ϵ is introduced to signify the presence of fast dynamics and nominally equals 1.0. We seek a reduced and zero-order boundary-layer solution about $\epsilon = 0$, in accordance with the procedures detailed in Refs. 2–4. Regarding h and γ as fast states is characteristic of energy state analysis for fighter and transport aircraft. Therefore, we adopt the same framework in this analysis. Considering both h and γ in the same time scale results in a two-point boundary-value problem. A feedback guidance law is obtained by expansion of the necessary conditions to first order.[11] In this regard, it should be noted that some studies have also considered analysis of h and γ dynamics on separate time scales,[12] which avoids linearization of the boundary-layer dynamics. Therefore, an additional set of guidance laws are possible beyond those presented here.

Singular-Perturbation Analysis

Reduced Problem

Setting $\epsilon = 0$ in Eqs. (14–16), the necessary conditions for optimality become

$$H_o = \lambda_\psi \dot{\psi} - \dot{E} = 0 \tag{19}$$

$$\gamma = 0, \qquad \lambda \cos\mu = -M \tag{20}$$

$$\mu_o,\ h_o = \arg\min_{h,\mu}\left\{\dot{\psi}/\dot{E}\right\} \tag{21}$$

It can be shown that this results in the following reduced solution:

$$\lambda_o = (1 + 2M_o^2)^{1/2} \tag{22}$$

$$\sin\mu_o = [(1 + M_o^2)/(1 + 2M_o^2)]^{1/2} \tag{23}$$

$$h_o = \arg\min_h\left\{V^2(1+M^2)^{1/2}\right\}\Big|_E = \text{const} \tag{24}$$

where M_o is the value of M for $h = h_o$. The quadrant for the bank angle in Eq. (23) is resolved based on the following inequalities:

$$0 < \mu_o < \pi/2 \text{ for } M_o < 0 \tag{25}$$

$$\pi/2 < \mu_o < \pi \text{ for } M_o > 0 \tag{26}$$

It can be seen from the preceding solution that M plays a crucial role in the solution process.

Since most of the energy is kinetic, V is weakly dependent on h for constant E. This can readily be seen from Eq. (9), where changes in h give rise to small changes in r. Thus, the minimization in Eq. (24) results in a value for M very close to zero. The interpretation is that the maneuver should be performed at an altitude at which gravitational and centrifugal forces nearly cancel one another. For M small, it can be seen from Eqs. (22) and (23) that the maneuver is performed at near-maximum L/D and at near-90 deg of bank angle. These results are in good agreement with the results in Ref. 8 for the AOTV problem. It has also been shown[5] that the reduced solution altitude profile, $h_o(E)$, closely resembles the altitude profile of Ref. 8 for the case of large changes in inclination angle.

Boundary-Layer Problem

Introducing the transformation $\tau = t/\epsilon$ and again setting $\epsilon = 0$, the necessary conditions in the boundary layer are

$$H_{BL} = \lambda_\psi^o \dot{\psi} + \lambda_h V \sin\gamma + \lambda_\gamma \dot{\gamma} - \dot{E} = 0 \tag{27}$$

$$\frac{\partial H_{BL}}{\partial L_1} = 0, \qquad \frac{\partial H_{BL}}{\partial L_2} = 0 \tag{28}$$

where λ_ψ^o is determined in the reduced solution from Eq. (19),

$$\lambda_\psi^o = \dot{E}^o/\dot{\psi}^o = -C_D^* V_o^2 (1 + M_o^2)^{1/2}/C_L^* \tag{29}$$

using the solutions for λ_o, μ_o, and h_o. In Eq. (28), L_1 and L_2 represent the horizontal and vertical components of lift coefficient

$$L_1 = \lambda \sin\mu, \qquad L_2 = \lambda \cos\mu \tag{30}$$

which are now used as control variables in place of λ and μ.

The first condition in Eq. (28) results in

$$L_1^* = (V_o/V)^2 (1 + M_o)^{1/2}/\cos\gamma \tag{31}$$

where M_o, V_o are the values of M and V corresponding to $h = h_o$ for the current value of E. This solution approaches the corresponding reduced solution as h approaches h_o.

The second condition in Eq. (28) yields

$$L_2^* = -(C_L^*/C_D^* V^2)\lambda_\gamma \tag{32}$$

which can also be shown to approach the reduced solution as h approaches h_o, where

$$\lambda_\gamma^o = C_D^* V_o^2 M_o / C_L^*, \qquad \lambda_h^o = 0 \tag{33}$$

The reduced solution for λ_γ in Eq. (33) follows immediately from Eqs. (16) and (32), with $L_2^* = -M_o(\epsilon\dot{\gamma} = 0$, in the reduced solution). The second condition in Eq. (33) is a consequence of the fact that h_o results from an unconstrained minimization of H^o. Note that λ_h^o satisfies the terminal boundary condition but λ_γ^o does not. This point will be addressed in the numerical results section.

Unfortunately, evaluation of λ_γ needed in Eq. (32) requires the solution of a two-point boundary-value problem. When close to the reduced solution, it may be possible to use Eq. (33), which results in the following expression for flight-path angle rate

$$\dot{\gamma} = C_L^* \rho S V (M \cos\gamma - V_o^2 M_o / V^2)/2m \tag{34}$$

For γ near zero and h near h_o, Eq. (34) simplifies to

$$\dot{\gamma} = C_L^* \rho S V_o (M - M_o)/2m \tag{35}$$

Use of Eqs. (31) and (32) with $\lambda_\gamma = \lambda_\gamma^o$ results in a guidance law in feedback form, which we denote as the SP1 solution.

Expansion of the Boundary-Layer Problem[11]

A second feedback solution can be obtained by considering an expansion of the boundary-layer necessary conditions of Eqs. (27) and (28), together with the state and costate dynamics, expressed in the stretched time scale $\tau = t/\epsilon$,

$$\frac{dh}{d\tau} = V \sin\gamma, \qquad \frac{d\lambda_h}{d\tau} = \frac{-\partial H_{BL}}{\partial h} \tag{36}$$

$$\frac{d\gamma}{d\tau} = C_L^* \rho S V (L_2 + M \cos\gamma)/2m, \qquad \frac{d\lambda\gamma}{d\tau} = -\frac{\partial H_{BL}}{\delta\gamma} \tag{37}$$

Substituting for L_1 and L_2 from Eqs. (31) and (32), Eqs. (36) and (37) are expanded about the reduced solutions equilibrium conditions

$$\bar{h} = h_o(E), \qquad \bar{\gamma} = 0 \tag{38}$$

$$\bar{\lambda}_h = 0, \qquad \bar{\lambda}_\gamma = \lambda_\gamma^o \tag{39}$$

This results in the following linear perturbation equations:

$$\begin{bmatrix} \delta h' \\ \gamma' \\ \lambda_h' \\ \delta\lambda_\gamma' \end{bmatrix} = \begin{bmatrix} 0 & V_o & 0 & 0 \\ K_1 & 0 & 0 & K_2 \\ K_3 & 0 & 0 & -K_1 \\ 0 & K_4 & -V_o & 0 \end{bmatrix} \begin{bmatrix} \delta h \\ \gamma \\ \lambda \\ \delta\lambda_\gamma \end{bmatrix} \tag{40}$$

where

$$K_1 = [V^2 r^2 - (\beta V^2 + \tilde{\mu})r + 2\beta\tilde{\mu}]/\beta V r^3 - 2\tilde{\mu}^2/V^3 r^4 - C_L^* S \tilde{\mu} M \rho / m V r^2 \tag{41}$$

$$K_2 = -C_L^* S \rho / 2mC_D^* V \tag{42}$$

$$K_3 = -\partial^2 H_{BL}/\partial h^2 \le 0 \tag{43}$$

$$K_4 = C_D^* S \rho V^3 (1 + 2M^2)/2m \tag{44}$$

The expressions in Eqs. (41-44) are evaluated at $h = h_o$, and β is the scale height in an exponential atmospheric model. The term in Eq. (43) is complicated to express analytically but can easily be evaluated numerically, taking into account that both H_{BL} and $\partial H_{BL}/\partial h$ evaluated at $h = h_o$ are zero.

The eigenvalues of Eq. (40) are arranged symmetrically about the imaginary axis and occur in complex conjugate pairs. In order to suppress the instability in the boundary-layer response, the state vector in Eq. (40) is expressed as

$$x = k_1 a + k_2 b \tag{45}$$

where $x^T = [\delta h, \gamma, \lambda_h, \delta\lambda_\gamma]$, and a,b are the real and imaginary parts of the eigenvectors associated with the stable eigenvalues. Knowing δh and γ, it is a simple exercise to solve for k_1, k_2, λ_h, and $\delta\lambda\gamma$. Then L_2^* in Eq. (32) can be evaluated for

$$\lambda_\gamma = \bar{\lambda}_\gamma + \delta\lambda_\gamma \tag{46}$$

Equations (31), (32), and (46) thus constitute a second feedback guidance law, which we term the SP2 solution.

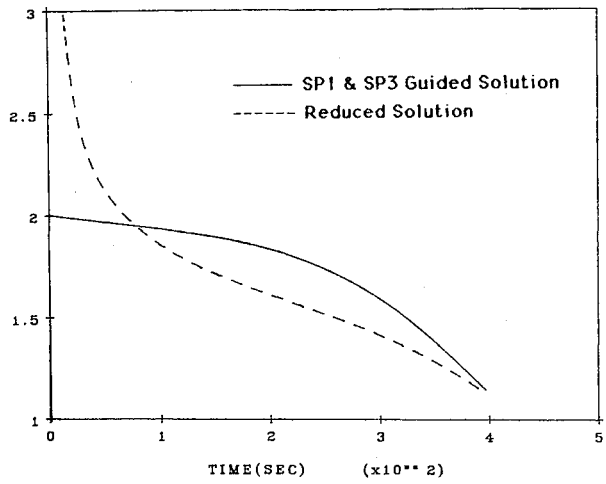

Fig. 1 Comparison of the SP1 and SP3 guided altitude profiles with the reduced solution.

Modeling Energy Rate Dynamics

If energy rate is modeled in the dynamics, the reduced model becomes a two-state problem, and the performance index is modified to minimize $-E(t_f)$. The Hamiltonian in this case is

$$H_o = \lambda_\psi \dot{\psi} + \lambda_E \dot{E} = 0, \qquad \lambda_E(t_f) = -1 \tag{47}$$

This gives rise to a two-point boundary-value problem in the reduced solution. However, an approximate integration of λ_E is possible in this case, based on the known properties of the optimal solution. Using Eq. (47), it is easy to demonstrate that

$$\dot{\lambda}_E = \frac{-\partial H_o}{\partial E} = \lambda_E C_D^* S \rho V(1+\lambda^2)/2m \tag{48}$$

Thus,

$$\frac{d\lambda_E}{d\psi} = (2C_D^*(1+\lambda^2)\cos\gamma/C_L^*\lambda\sin\mu)\lambda_E \simeq (2C_D^*/C_L^*)\lambda_E \tag{49}$$

where the approximations $\lambda \simeq 1$, $\mu \simeq \pi/2$, $\gamma \simeq 0$ have been employed. Integration of Eq. (49) results in

$$\lambda_E(\psi) \simeq -\exp\left\{-2C_D^*(\psi_f - \psi)/C_L^*\right\} \tag{50}$$

Comparing the Hamiltonian expressions in Eqs. (19) and (47), it can be seen that modeling E as constant in the dynamics amounts to the approximation $\lambda_E = -1$. Equation (50) represents an improvement, but the approximation $\lambda_E = -1$ is apparently accurate for high L/D vehicles. As to its effect on the reduced solution, Eqs. (22–26) remain the same. The reduced costate solutions become

$$\lambda_\psi^o = -\lambda_E C_D^* V_o^2(1+M_o^2)^{1/2}/C_L^* \tag{51}$$

$$\lambda_h^o = 0, \qquad \lambda_\gamma^o = \lambda_E C_D^* V_o^2 M_o/C_L^* \tag{52}$$

Note that the ψ and γ costate solutions are now simply multiplied by λ_E. The boundary-layer solution for L_1^* in Eq. (31) remains the same, but Eq. (32) becomes

$$L_2^* = -(C_L^*/C_D^* V^2)\lambda_\gamma/\lambda_E \tag{53}$$

Thus, the SP1 control solution, which uses $\lambda_\gamma = \lambda_\gamma^o$, remains unchanged when E is modeled in the dynamics, since λ_E is canceled when λ_γ^o from Eq. (52) is substituted in Eq. (53). The SP2 solution, on the other hand, is affected in that several of the matrix elements in Eq. (40) are changed. In particular, K_2 and K_4 are divided by λ_E, and H_{BL}, used in the computation K_3, becomes

$$H_{BL} = \lambda_\psi \dot{\psi} + \lambda_h V \sin\gamma + \lambda_\gamma \dot{\gamma} + \lambda_E \dot{E} \tag{54}$$

We will refer to the control solution obtained with these modifications as the SP3 solution.

Numerical Results

A numerical study was performed to evaluate the performance of the three guidance laws derived in the preceding section. The parameter values chosen to approximate the vehicle studied in Ref. 8 are as follows:

$$C_{D0} = 0.032, \quad S = 125.8 \text{ ft}^2, \quad K = 1.4, \quad m = 331.5 \text{ slugs}$$

The initial conditions were chosen to match the 40-deg heading change maneuver of Ref. 8, where the sensible atmosphere was defined to begin at an altitude of 200,000 ft. The corresponding entry velocity and flight-path angles are $V(0) = 25{,}945$ ft/s and $\gamma(0) = -0.148$ deg. A simple exponential atmospheric model was defined using the standard atmospheric data for air density at altitudes of 10^5 and 2×10^5 ft. All of the comparisons are for a 40-deg heading change.

Figure 1 compares the reduced solution altitude profile obtained from Eq. (24) with the SP1 and SP3 guided solution profiles, which on this scale are identical. A similar comparison is given for the SP2 guided solution in Fig. 2. Note that the reduced solution provides a reasonable altitude profile except at high energies near the initial time. However, this region of the solution is of little interest since the air density is negligibly small. In any case, it is not physically possible to follow this profile (recall that h is used as a control variable in the reduced

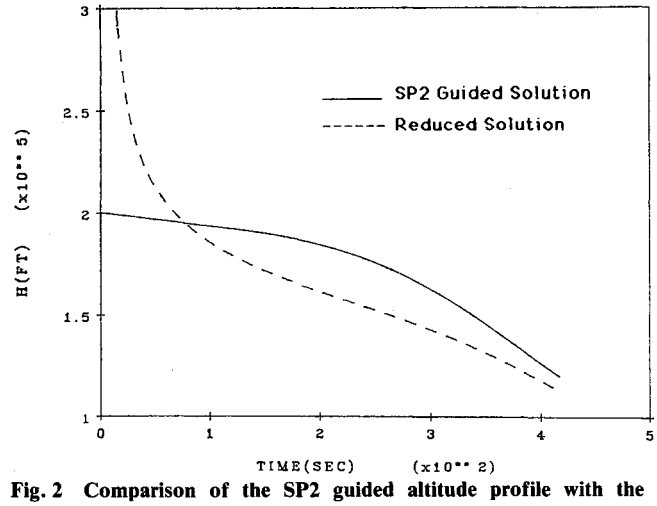

Fig. 2 Comparison of the SP2 guided altitude profile with the reduced solution.

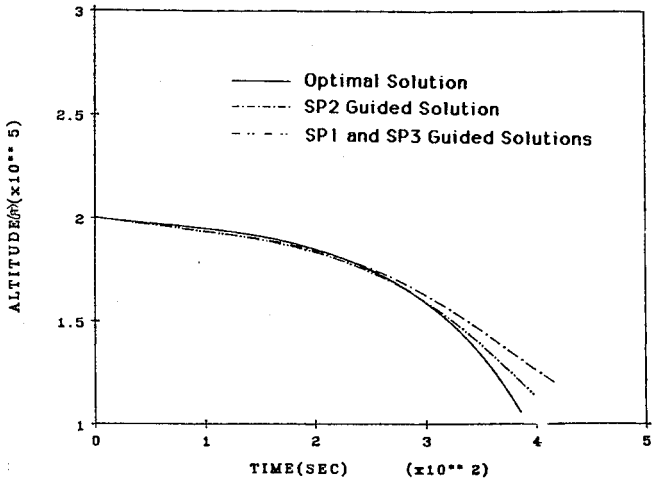

Fig. 3 Comparison of the guided altitude profiles with the true optimal solution.

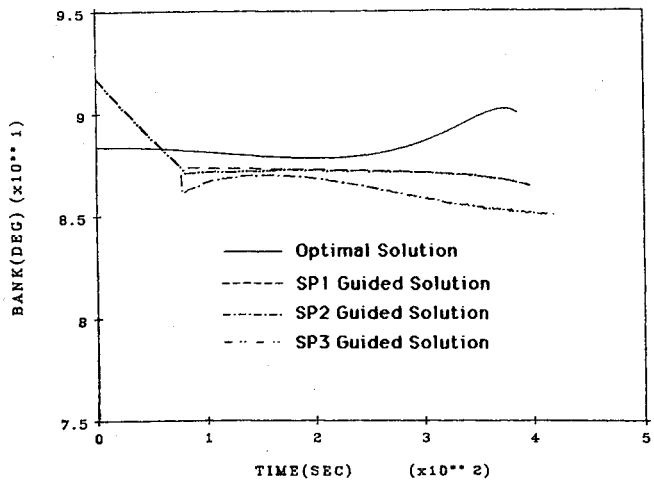

Fig. 4 Bank-angle profiles.

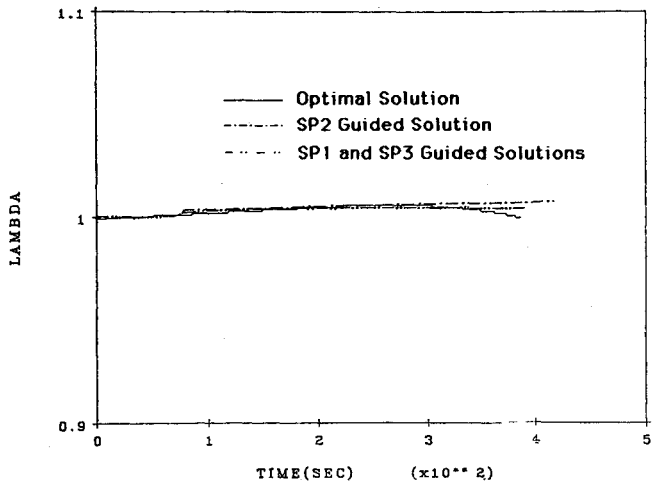

Fig. 5 Normalized lift coefficient profiles.

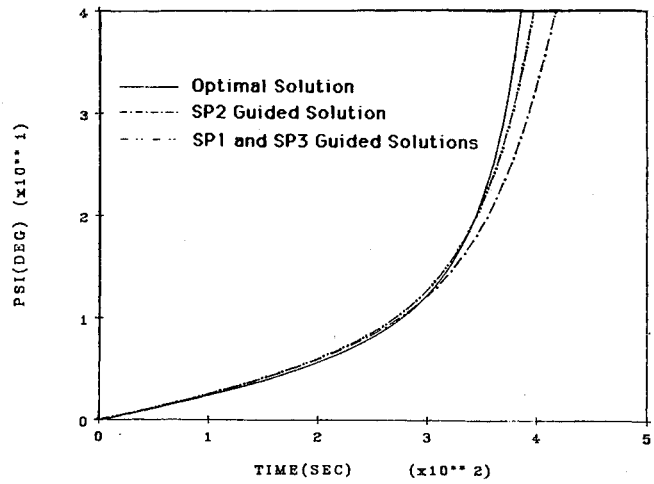

Fig. 6 Heading profiles.

Table 1 Comparison of final conditions

Guidance	t_f	$E_f \times 10^8$	$\Delta E \times 10^8$
Optimal	358.6	−4.813	1.510
SP1	397.0	−4.813	1.510
SP2	415.8	−4.814	1.511
SP3	398.0	−4.813	1.510

solution). Thus, it was decided to maintain $\lambda = 1$ and $\lambda \cos\mu = -M$ ($\dot{\gamma} = 0$) until $h_o(E)$ falls below the current altitude.

In order to evaluate the optimality of these solutions, an optimal solution was numerically computed using a multiple shooting algorithm.[9] The four-state model in Eqs. (1-4) was used to define the dynamics. The SP1 guided solution was used as an initial guess for the state time histories, and the reduced solutions in Eqs. (29), (39), and (50) were used as an initial guess for the costate time histories. The solution converged to a relative precision of 10^{-12} in eight iterations. The value of the Hamiltonian was constant and essentially zero, considering the relative precision accuracy required for convergence. This served as an independent check on the accuracy of the solution.

Figure 3 compares the optimal altitude profile with the profiles that result from the three guided solutions. Note that the optimal solution dips slightly more into the atmosphere near the end and, consequently, results in slightly decreased flight time. The corresponding control time histories and heading profiles are compared in Figs. 4-6. Note that, in Fig. 4, the optimal bank angle at the final time is 90 deg, which follows from Eq. (32) and the fact that $\lambda_\gamma(t_f) = 0$. In the context of singular-perturbation theory, this gives rise to a terminal boundary layer that must be solved backward in time. Since this was ignored in our analysis, the guided solutions approach the condition in Eq. (33) instead. This explains the departure in the altitude profiles in Fig. 3. It is apparent that this effect is a minor one. In any case, the dip in the optimal profile may not be desirable from a practical standpoint.

It may be somewhat surprising at this point that the SP1 and SP3 solutions are nearly identical. However, recall that the SP1 solution is not sensitive to the approximation that E is modeled as constant in the dynamics. The SP3 solution corrects the SP2 solution for this modeling approximation and results in essentially the same solution as the SP1 solution. This fact also justifies the use of approximation $\lambda_\gamma = \lambda_\gamma^o$ in the SP1 solution. Table 1 compares the energy loss for all the solutions and shows that the three guided solutions produce essentially optimal performance. The energy loss for the SP1 and SP3 solutions is indistinguishable from the optimal solution to four significant places, whereas the energy loss for the SP2 solution is 0.06% greater.

Conclusions

It has been demonstrated that the use of model order reduction and singular-perturbation analysis is useful in deriving feedback guidance algorithms for hypervelocity vehicles. Although the problem formulation was simplified to avoid terminal constraints on altitude and flight-path angle, the results do indicate that these methods are effective in developing suboptimal guidance strategies.

Acknowledgment

This research was supported by NASA Langley Research Center under Grant NAG-1-660.

References

[1]Bryson, A. E., Desai, M. N., and Hoffman, W. C., "Energy-State Approximation in Performance Optimization of Supersonic Aircraft," *Journal of Aircraft*, Vol. 6, No. 6, 1968, pp. 481-488.

[2]Calise, A. J., "Singular Perturbation Methods for Variational Problems in Aircraft Flight," *IEEE Transactions on Automatic Control*, Vol. AC-21, No. 3, June 1976, pp. 345-353.

[3]Calise, A. J., "Extended Energy Management Methods for Flight Performance Optimization," *AIAA Journal,* Vol. 15, March 1977, pp. 314–321.

[4]Calise, A. J., "Singular Perturbation Techniques for On-Line Optimal Flight-Path Control," *Journal of Guidance and Control,* Vol. 4, No. 4, 1981, pp. 398–405.

[5]Calise, A. J., "Singular Perturbation Analysis of the Atmospheric Orbital Plane Change Problem," *Journal of the Astronautical Sciences,* Vol. 36, Jan.–June 1988, pp. 35–77.

[6]Joosten, B. K., and Pierson, B. L., "Minimum-Fuel Aerodynamic Orbital Plane Change Maneuvers," AIAA Paper 81-0167, Jan. 1981.

[7]Hull, D. G., and Speyer, J. L., "Optimal Reentry and Plane-Change Trajectories," *Journal of the Astronautical Sciences,* Vol. 30, No. 2, 1982, pp. 117–130.

[8]Hull, D. G., Giltner, J. M., Speyer, J. L., and Mapar, J., "Minimum Energy-Loss Guidance for Aero-Assisted Orbital Plane Change," *Journal of Guidance, Control, and Dynamics,* Vol. 8, No. 4, 1985, pp. 487–493.

[9]Burlish, R., "The Multiple Shooting Method for Numerical Solution of Nonlinear Boundary Value Problems and Optimal Control Problems" (in German), Carl-Cranz-Gessellschaft, Heidelberg, FRG, Tech. Rept., 1971.

[10]Calise, A. J., and Bae, G., "A Near Optimal Guidance Algorithm for Aero-Assisted Orbit Transfer," AIAA Paper 88-4175, Aug. 1988.

[11]Ardema, M. D., "Linearization of the Boundary Layer Equations of the Minimum Time-To-Climb Problem," *Journal of Guidance and Control,* Vol. 2, No. 5, 1979, pp. 434–436.

[12]Calise, A. J., "Optimization of Aircraft Altitude and Flight-Path Angle Dynamics," *Journal of Guidance, Control, and Dynamics,* Vol. 7, No. 1, 1984, pp. 123–125.